Numerical investigation of the effect of improved endochronic constitutive model on rock material deformation under cyclic loading

Jian Ming Huang[a] (iD), **Shi li Hu[a]** (iD), **Lu Jun Chen[a]** (iD), **Xiang Liu[a]** (iD), **Wei Zeng[a]*** (iD)

[a] School of Architectural and Surveying& Mapping Engineering, JiangXi University of Science and Technology, Ganzhou,China.
Email: huang_19962020@163.com, hslqhd@163.com, 378652342@qq.com, liuxiang5511@163.com, 1368960034@qq.com
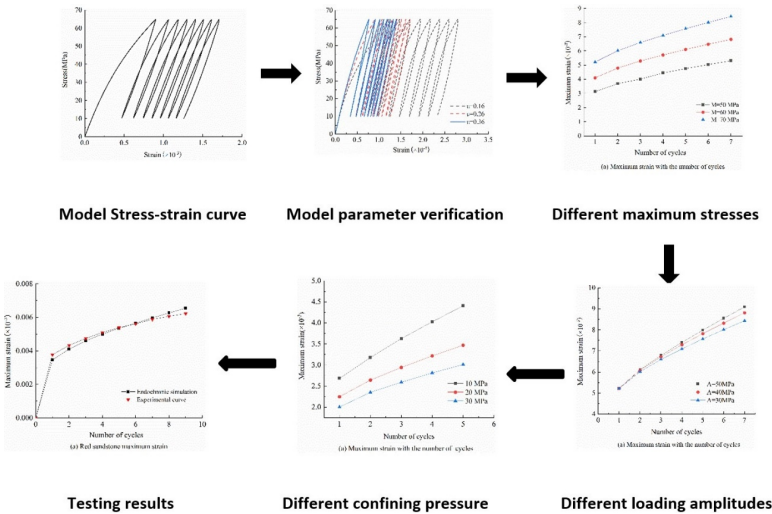
* Corresponding author

Abstract

Rock materials are often subjected to cyclic loads during construction. A full understanding of the deformation behavior of rock under cyclic loads is of great significance in engineering. In this study, by using the endochronic constitutive model proposed by Valanis, the reinforcement function form and constitutive parameters of the endochronic model are improved. An endochronic plasticity constitutive program for rock based on the finite element method is used to study the mechanical properties of rock under different cyclic loading conditions (of maximum loading stress, amplitude, and confining pressure), and through the use of red sandstone, marble, and basalt, experimental and simulation results are compared to verify the model. The results show that the theory can better simulate the hysteresis loop width and cumulative plastic strain of rock under cyclic loading and, under different loading conditions, the numerical simulation results are consistent with the actual rock experimental law. Therefore, the endochronic plasticity constitutive model in this study can be applied to investigate the influence of cyclic loading on the dynamic deformation behavior of rock.

Keywords
cyclic loading; endochronic constitutive mode; residual strain; finite element method

Graphical Abstract

Model Stress-strain curve   Model parameter verification   Different maximum stresses

Testing results   Different confining pressure   Different loading amplitudes

Numerical investigation of the effect of improved endochronic constitutive model on rock material deformation under cyclic loading

Jian Ming Huang et al.

1 INTRODUCTION

Dams, underground caverns, slopes and other rock projects are often influenced by earthquakes, resulting in damage or even destruction of engineering structures, which directly threatens construction and life safety (Khaledi, K et al., 2016). Generally, scholars regard earthquakes as cyclic loads (Liu, Y et al., 2017), and it is known that the mechanical response of rocks under cyclic dynamic loads is significantly different from that under static loads (Xiao et al., 2009). Therefore, it is necessary to study the mechanical properties of rocks under cyclic loading and the corresponding constitutive model, which is of great significance for the geotechnical stability calculation under seismic loading.

The mechanical properties of rocks under cyclic load and different loading conditions of cyclic load have been studied in great depth by many scholars through experiments. For example, rocks have Masing effect and ratchet effect under cyclic loading, and different mechanical responses in terms of amplitude, confining pressure, maximum loading stress and other cyclic loading conditions (Attewell and Farmer 1973; Zhou et al., 2015; Badge and Petroš 2005; Deng et al., 2017; Liu et al., 2012; Momeni A et al., 2015; Fuenkajorn and Phueakphum 2010; Ge et al., 2003; Xiao et al., 2007). The above experimental results show that the constitutive model of rocks under different cyclic loading conditions is more complex, and the mathematical expression of the constitutive model of rocks under cyclic loading conditions remains a difficult problem in the field of geotechnical engineering. The classic elastoplastic theory can well describe the mechanical behaviors of rocks under static loading conditions, but it can not accurately describe the dynamic response of rocks (Liu et al., 2014). Di proposed a binary medium constitutive model which can better reflect the ratchet effect of rocks under cyclic loading, but the simulation results of the hysteretic effect of rocks are still not satisfactory (Di et al., 2020). Zhou applied the sub-loading surface model to rock materials and obtained good simulation results, but the strain rate effect was not considered for the rock dynamic problem (Zhou et al., 2015). In addition, PM model and fatigue constitutive model, etc. have more experimental parameters, and their practicality in actual engineering needs to be improved (Carmeliet J and Abeele KEVD 2002; Lin et al., 2020). Compared with the above models, the endochronic model is better for the dynamic response of rocks under cyclic loading, so the endochronic model is chosen as the basis for the theoretical research in this study. Valainis first applied the endochronic theory to metallic materials and studied the deformation of metallic materials under cyclic loading, while Bazant first applied the endochronic theory to rock materials (Valanis 1971; Bazant, ZP and Shieh, CL 1980). But the rock endochronic model proposed by Bazant contains too many parameters without practical physical meaning, which is not conducive to experimental simulations in different rock situations. Subsequently, many scholars applied the endochronic theory to the experimental studies of different materials such as concrete , soil and coal containing gas, and good experimental results were also obtained (Wang and Song 2007; Jeremiah M et al., 2019; Yin et al., 2009). However, the large number of parameters without actual physical meaning in the endochronic constitutive reinforcement function has always been a difficult problem in the study of endochronic theory.

Therefore, on the basis of the endochronic constitutive model by Bazant, the endochronic constitutive model of rocks under different cyclic loading is studied in this paper, and the number of parameters in the endochronic model is reduced, proposing an improved endochronic constitutive model. Moreover, based on the finite element method, a related calculation procedure was written using the improved endochronic constitutive model (Shimbo, 2017; Tejchman and Bobinski 1996; Xiong et al., 2017; Cheng et al., 2020; Cheng et al., 2021; Han et al., 2008). Through numerical simulation experiments, the improved endochronic constitutive model simulation upon the Masing effect and ratchet effect of rocks is studied, and the physical meaning of the endochronic constitutive model parameters is discussed. By changing the cyclic loading conditions such as maximum loading stress, amplitude, confining pressure and rock types, the mechanical behaviors of rocks under the above different loading conditions were systematically analyzed, which verified the rationality and feasibility of the model in this study.

2. BASIC PRINCIPLES OF ENDOCHRONIC PLASTICITY CONSTITUTIVE THEORY

2.1 Endochronic theory

Endochronic theory was proposed by Valanis (Valanis 1971). Its basic concept can be expressed as follows: The current stress state at any point in plastic and viscoplastic materials is a function of the entire temperature and deformation in the field at that point. It is very important that the deformation history be measured by an endochronic time that depends on the material properties and the degree of deformation, rather than the conventional Newton time, to measure the history of irreversible deformation. The object is regarded as a thermodynamic system, and the plastic deformation of the material is an irreversible process; therefore, plastic deformation is regarded as an irreversible change state of thermodynamics; the concept of yield surface as the prerequisite for its theoretical development is not

Numerical investigation of the effect of improved endochronic constitutive model on rock material deformation under cyclic loading

Jian Ming Huang et al.

considered, but the existence of the posterior behavior of the yield surface is not excluded (Watanabe and Atluri, 1985). Instead, the kinematic hardening and isotropic kinematic hardening in the concept of the yield surface are taken as special cases derived from the simplification of endochronic theory. Compared with traditional plastic theory, endochronic theory can better reflect the hysteretic effect and plastic cumulative strain of rock under cyclic loading.

2.2 Derivation of endochronic theory

The internal energy of the rock can be expressed as

$$W = (\varepsilon_{ij}, q_\alpha, T) \qquad (\alpha = 1, 2, 3 \ldots, m) \tag{1}$$

where W is internal energy, q_α is the internal variable, T is the temperature, and φ is the state function. Its total differential form is given by (Li and Fu 1991)

$$dW = \frac{\partial W}{\partial \varepsilon_{ij}} d\varepsilon_{ij} + \frac{\partial W}{\partial q_\alpha} dq_\alpha + \frac{\partial W}{\partial T} dT \tag{2}$$

For any irreversible system undergoing a thermodynamic process, the state function of entropy can be expressed as

$$\eta = (\varepsilon_{ij}, q_\alpha, \theta) \tag{3}$$

where $\theta = \theta(\varepsilon_{ij}, T)$ is the thermodynamic temperature scale T. According to the definition of the Helmholtz free energy function,

$$\psi = W - \theta \eta \tag{4}$$

Because ψ is also a state function,

$$\sigma_{ij} = \frac{\partial \psi}{\partial \varepsilon_{ij}} \tag{5}$$

and

$$\eta = -\frac{\partial \psi}{\partial \theta} \tag{6}$$

From the above formula, the following can be derived:

$$d\psi = \frac{\partial \psi}{\partial \varepsilon_{ij}} d\varepsilon_{ij} + \frac{\partial \psi}{\partial q_\alpha} dq_\alpha - \frac{\partial \psi}{\partial T} dT \tag{7}$$

As assumed by Kelvin, under isothermal conditions, the free energy in the region cannot be increased, and we can obtain

$$-\frac{\partial \psi}{\partial q_\alpha} dq_\alpha \geq 0 \tag{8}$$

Because the changes in the internal variables are completely independent, a generalized friction force is introduced under the condition of irreversible deformation, and the friction force can be expressed as

Numerical investigation of the effect of improved endochronic constitutive model on rock material deformation under cyclic loading

Jian Ming Huang et al.

$$Q_{ij}^{(\alpha)} = -\frac{\partial \psi}{\partial q_{ij}^{(\alpha)}} \tag{9}$$

$$Q_{ij}^{(\alpha)} dq_{ij}^{(\alpha)} \geq 0 \tag{10}$$

For rock materials, it can be assumed that the generalized friction force $Q_{ij}^{(\alpha)}$ is proportional to the rate of change of the internal variable, $dq_{ij}^{(\alpha)}/dz$, and thus the following can be obtained:

$$Q_{ij}^{(\alpha)} = b_{ijkl}^{(\alpha)} \frac{dq_{ij}^{(\alpha)}}{dz}$$

where $b_{ijkl}^{(\alpha)}$ is the generalized coefficient of friction. Substituting Eq. (11) into Eq. (10), we get

$$\frac{\partial \psi}{\partial q_{ij}^{(\alpha)}} + b_{ijkl}^{(\alpha)} \frac{dq_{ij}^{(\alpha)}}{dz} = 0 \tag{12}$$

Furthermore, the constraint conditions on the internal variable group were obtained as described above. Eq.(1) can be expanded in a Taylor series to obtain

$$\psi = \frac{1}{2} A_{ijkl} \varepsilon_{ij} \varepsilon_{kl} + B_{ijkl} \varepsilon_{ij} q_{ijkl}^{\alpha} + \frac{1}{2} \sum_{\alpha} C_{ijkl} q_{ij}^{\alpha} q_{kl}^{\alpha} + D_{ij} T \varepsilon_{ij} + I_{ij} T q_{ij}^{\alpha} + \frac{1}{2} FT^2 \tag{13}$$

where A_{ijkl}, B_{ijkl}, C_{ijkl}, D_{ij}, I_{ij}, and F are the generalized parameters of the material. For rock materials, under the condition of small isothermal deformation, from Eqs. (5), (8), and (12), the displayed endochronic constitutive equation can be obtained as

$$s_{ij} = 2 \int_0^z \mu(z - z') \frac{\partial e_{ij}^p}{\partial z'} dz' \tag{14}$$

with

$$\mu(z) = \sum_{i=1}^{\infty} M_i \exp(-\alpha_i z) \tag{15}$$

where $\mu(z)$ is the kernel function of the material, z is the endochronic scalar scale, e_{ij}^p is the plastic deviatoric strain tensor, and s_{ij} is the deviatoric stress tensor. To meet the weak singularity and integrability requirements, the coefficients α_i and M_i need to satisfy

$$\sum_{i=1}^{\infty} M_i = \infty, \qquad \sum_{i=1}^{\infty} \frac{M_i}{\alpha_i} \neq \infty \tag{16}$$

A schematic of endochronic theory in strain space is shown in Fig. 1. The distance between two adjacent points along the strain path can be expressed as follows:

$$d\zeta^2 = P_{ijkl} d\varepsilon_{ij} d\varepsilon_{kl} \tag{17}$$

Numerical investigation of the effect of improved endochronic constitutive model on rock material deformation under cyclic loading

Jian Ming Huang et al.

where ζ is the scale of the endochronic theory tensor in three-dimensional strain space and P_{ijkl} is a fourth-order positive definite tensor that depends on the properties of the material.
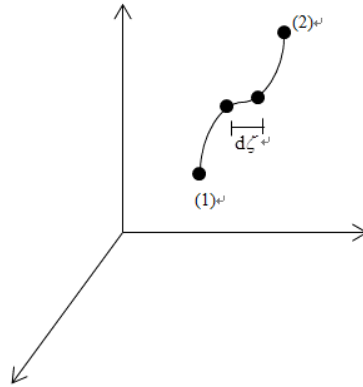

Figure 1. Strain space and stress path

The endochronic tensor scale $d\zeta$ and the endochronic scalar scale z described in Eqs. (17) can be obtained by the following transformation:

$$dz = \frac{d\zeta}{f(\zeta)} \tag{18}$$

where $f(\zeta)$ is the strengthening function under a generalized friction force. For the endochronic scalar scale, without considering the coupling effect of plastic deviator strain and volume strain, the definition of the endochronic tensor scale proposed in reference (Mo 1988; Zhang et al., 2015) is as follows:

$$d\zeta = \left\| de_{ij}^p \right\| \tag{19}$$

$$de^p = de_{ij} - \frac{ds_{ij}}{2G_0} \tag{20}$$

$$de_{ij} = d\varepsilon_{ij} - \frac{1}{3}d\varepsilon_{kk}\delta_{ij} \tag{21}$$

According to Eq. (14), its differential form is as follows:

$$ds_{ij} = 2G_0 de_{ij} - s_{ij}dz \tag{22}$$

where G_0 is the elastic shear modulus, $\|\cdot\|$ is the norm in Euclidean space, and e^p, e_{ij}, and s_{ij} are the plastic deviatoric strain, deviatoric strain tensor, and deviatoric stress tensor, respectively. To facilitate computer analysis and calculation, Eq. (22) is transformed into a matrix form of the incremental endochronic constitutive equation as follows:

$$\{d\sigma\} = \left[D_{ep}\right]\{d\varepsilon\} - \left\{dH^p\right\} \tag{23}$$

The specific form of the above matrix form in the case of three dimensions is given by the following formulas:

$$\{d\sigma\}^T = \left\{d\sigma_x, d\sigma_y, d\sigma_z, d\tau_{xy}, d\tau_{yz}, d\tau_{zx}\right\} \tag{24}$$

$$\{d\varepsilon\}^T = \left\{d\varepsilon_x, d\varepsilon_y, d\varepsilon_z, d\gamma_{xy}, d\gamma_{yz}, d\gamma_{zx}\right\} \tag{25}$$

Numerical investigation of the effect of improved endochronic constitutive model on rock material deformation under cyclic loading

Jian Ming Huang et al.

$$\{dH^p\} = \{dH_x^p \ dH_y^p \ dH_z^p \ dH_{xy}^p \ dH_{yz}^p \ dH_{zx}^p\}$$
$$= (s_x \ s_y \ s_z \ s_{xy} \ s_{yz} \ s_{zx})\Delta Z$$

(26)

$$[D_{ep}] = \begin{bmatrix} A_1 & A_2 & A_2 & 0 & 0 & 0 \\ A_2 & A_1 & A_2 & 0 & 0 & 0 \\ A_2 & A_2 & A_1 & 0 & 0 & 0 \\ 0 & 0 & 0 & A_3 & 0 & 0 \\ 0 & 0 & 0 & 0 & A_3 & 0 \\ 0 & 0 & 0 & 0 & 0 & A_3 \end{bmatrix}$$

(27)

where $A_1 = K_0 + \dfrac{4}{3}G_0$, $A_2 = K_0 + 2G_0$, and $A_3 = 2G_0$.

Under the action of a compressive load, the inelastic strain accumulated in a cycle decreases as the process continues. The following enhanced function form is proposed according to the test data fitting:

$$f(\zeta) = u \times (1 - 0.55\exp^{\zeta}) \times \left(\frac{\sigma_3}{1 + (J_2)^{1/4}}\right)^{\beta}$$

(28)

σ_3 is the third principal stress, J_2 is the second invariant of the strain deviation, and u and β are the model parameters.

2.3 Finite element implementation of the endochronic plasticity model

According to the above theory, we use the C language to compile the endochronic plasticity finite element program. The program uses the initial stress method to calculate. From the elastic system with known initial stress, the following formulas can be obtained using the principle of virtual work:

$$[K]\{\sigma\} = \{P\} + \{dP_0\}$$

(29)

$$\{dP_0\} = -\int [B]^T \{\sigma\} dV$$

(30)

where $\{dP_0\}$ is the load-correction term of the initial stress effect and $[B]$ is the strain matrix.

The program is initially loaded through the initial loading for linear elastic calculation, and the third principal stress and the second strain invariant of the element are calculated to determine the strengthening function $f(\zeta)$; in the nth step, the corresponding endochronic increment and plastic strain are calculated using Eqs. (18) and (19), and then the new plastic stiffness matrix is calculated using Eq. (23) to judge whether the new and old ones exceed the convergence criterion. The initial stress method is used to compare the calculated element stress with the initial stress and determine its convergence criterion by controlling the accuracy of the unbalanced force. The specific process is shown in Fig. 2, where the difference between the rock constitutive acceleration method in this study and the traditional algorithm is that the concept of yield surface is not used, which avoids the shortcoming of the difficulty in determining the yield surface for materials such as a rock.
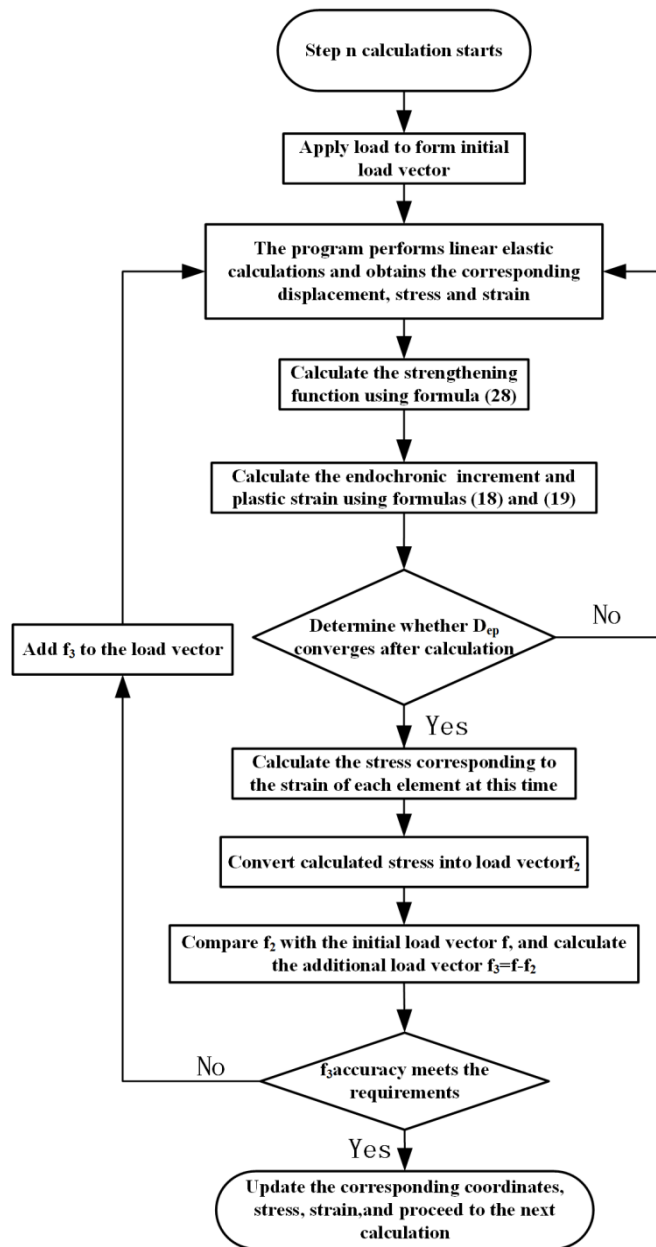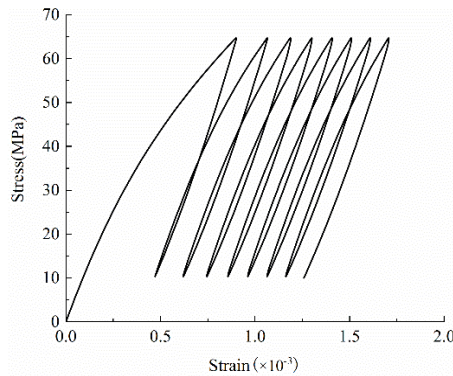
Numerical investigation of the effect of improved endochronic constitutive model on rock material deformation under cyclic loading

Jian Ming Huang et al.

Figure 2. Flowchart of the elastoplastic program

3 STRENGTHENING FUNCTION PARAMETER FOR THE ENDOCHRONIC CONSTITUTIVE MODEL

For the improved endochronic plastic model, the parameters of the model are E, v, u, M_i, α_i, and β. E and v are the elastic modulus and Poisson's ratio of the material, respectively. According to the literature (Yin et al., 2009), the values of M_i and α_i are determined according to the collection of the stress-strain curve close to the origin. u and β are specific parameters of the endochronic model. According to the cyclic loading experimental data, the parameters β and u can be obtained by nonlinear fitting. In the curve simulation process, the selection of these two parameters has a certain influence on the curve simulation. Therefore, it is necessary to analyze these two values. We selected a rock cube with a size of 100 mm × 100 mm × 100 mm and applied a triangular waveform cyclic load to the test block without confining pressure. The rock cube will was divided into a tetrahedral mesh. The upper limit of the applied load was 65 MPa, the lower limit of the load was 10 MPa, and the number of loading times was 8. Table 1 lists the material parameters used in the simulation experiment.
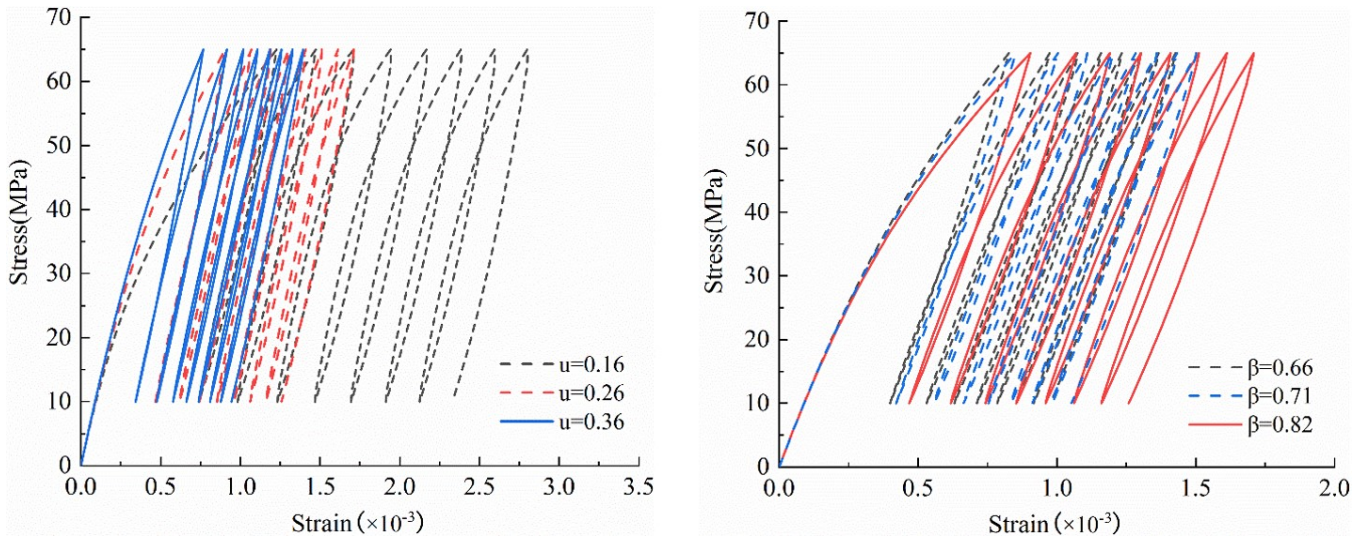
Numerical investigation of the effect of improved endochronic constitutive model on rock material deformation under cyclic loading

Jian Ming Huang et al.

Table 1. Parameters of the model material

E (Pa)	v	u	β	M_i	α_i
2.5×10^9	0.2	0.26	0.71	2.6×10^8	2×10^2

Figure 3. Stress–strain curve

As shown in Fig. 3, during loading and unloading, the rock material undergoes plastic deformation. The stress–strain curve formed a hysteresis loop. As the number of cycles increased, the material's cumulative plastic strain gradually increased. The above numerical simulation results better reflect the Masing effect and the ratchet effect of the rock, and the inelastic strain accumulated in one cycle of the rock decreases with an increase in the number of cycles. Therefore, using the above simulation experiment parameters as the experimental base point, the influence of parameters u and β on the modified endochronic model is discussed.

Figure 4. Effect of parameters on the endochronic constitutive model

As shown in Fig. 4, as the value of u decreases, the plastic modulus gradually decreases, indicating that, with the decrease in u, the greater the cumulative plastic strain generated, the more obvious the ratchet effect of the rock (Zhou et al., 2015). β has little effect on the loading slope of the curve, but, as β increases, its hysteresis loop gradually increases, reflecting the Masing effect of the rock under cyclic loading, but the cumulative plastic strain rate is not significantly different.

4 CHARACTERISTICS OF THE IMPROVED ENDOCHRONIC CONSTITUTIVE MODEL

4.1 Influence of maximum load under cyclic loading

According to the literature (Momeni et al., 2015; Ma et al., 2013), the stress level of a cyclic load is one of the main factors affecting rock deformation in the case of constant amplitude. When the amplitude of the cyclic load is 30 MPa,

Numerical investigation of the effect of improved endochronic constitutive model on rock material
deformation under cyclic loading

Jian Ming Huang et al.

and the maximum load is set to 50, 60, and 70 MPa, respectively, the stress–strain curve under the cyclic load is shown in Fig. 5. Fig. 6 illustrates the changes in the maximum axial strain and residual strain under different maximum load stress conditions. As shown in Fig. 5, with an increase in the maximum loading stress, the axial strain and residual strain corresponding to the rock both increase, and the deformation of the rock increases rapidly in the first loading cycle and slowly in the subsequent loading process. Figs. 6(a) and 6(b) show the effect of the maximum load stress on the maximum axial strain and residual strain. With an increase in the maximum load stress, the residual deformation of the rock and the maximum axial strain increased approximately linearly. When the maximum load stress increased from 50 to 70 MPa, in the last cycle, the maximum axial strain increased from 0.00531 to 0.008435, and the residual strain increased from 0.004075 to 0.007245.
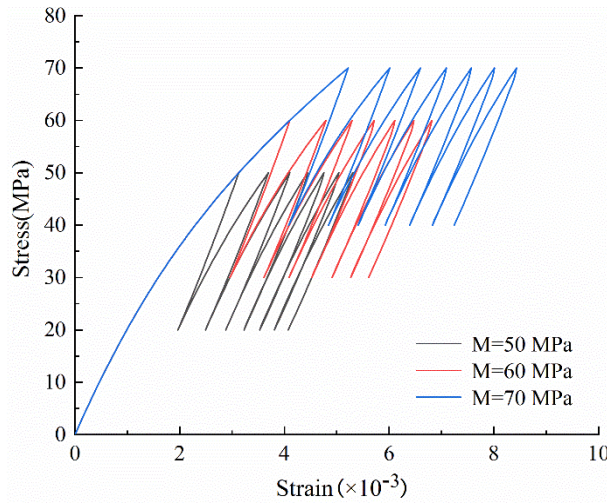

Figure 5. Stress–strain curves under different maximum stresses

(a) Maximum strain with the number of cycles
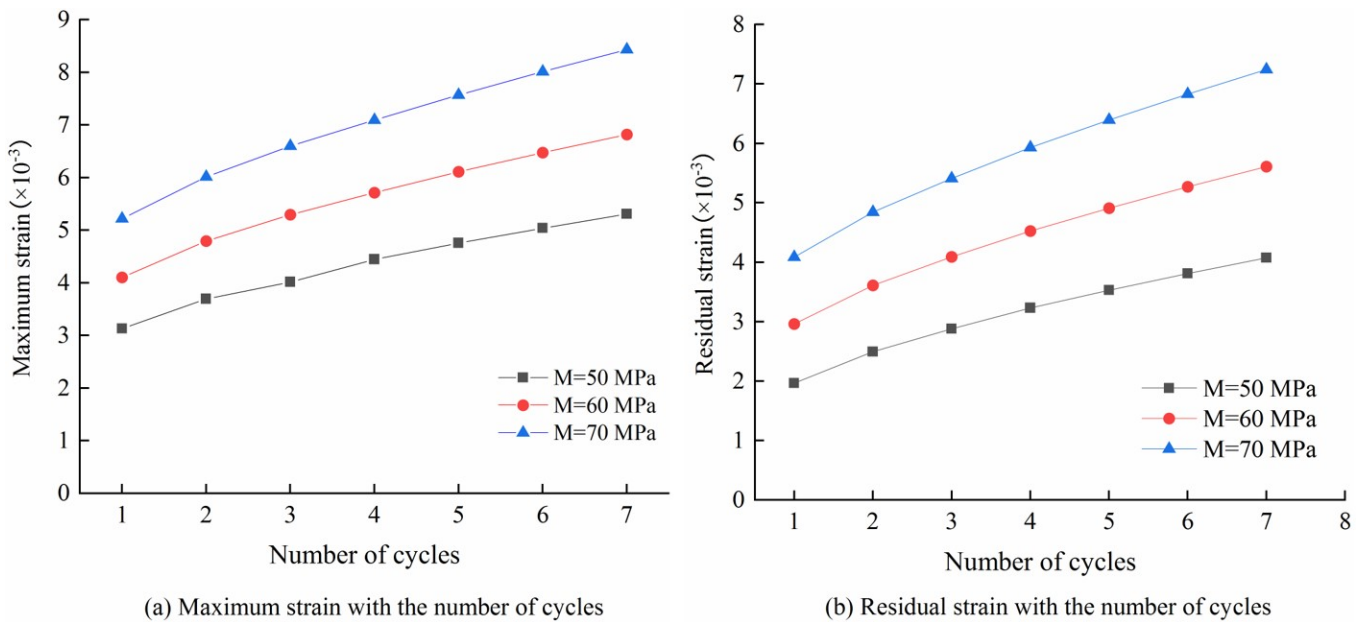
(b) Residual strain with the number of cycles

Figure 6. Variation in strain with cycle times under different maximum stresses

The above phenomenon is described by the rock fracture mechanism in the literature (Momeni et al., 2015); when the maximum load stress of rock under a cyclic load increases gradually, the internal cracks expand more easily, and, with the formation of cracks, the degree of rock damage increases; therefore, the maximum strain axial strain and residual strain of the rock increase with the increase in the maximum load stress. The phenomenon described in the numerical simulation results in this study is consistent with the actual deformation phenomenon of rock materials under different maximum loadings.

Numerical investigation of the effect of improved endochronic constitutive model on rock material deformation under cyclic loading

Jian Ming Huang et al.

4.2 Influence of loading amplitude under cyclic loading

In the case of a fixed maximum load of 70 MPa, three sets of different amplitude data were selected for experiments to analyze the deformation of the rock under different amplitude conditions. The stress–strain curves of the rock under different amplitudes are shown in Fig. 7, and the residual strain and maximum axial strain of the rock under different load amplitudes are shown in Fig. 8. From the stress–strain diagram and the residual strain diagram, one can observe that, as the amplitude increases, the residual strain gradually decreases, and the residual strain is inversely proportional to the amplitude, which is consistent with the experimental results in the literature (Wang et al., 2020; Wang, YS et al., 2016). When the amplitude increased from 30 to 50 MPa, the maximum axial strain in the last cycle increased from 0.00843 to 0.0091, while the residual strain decreased from 0.00724 to 0.007.
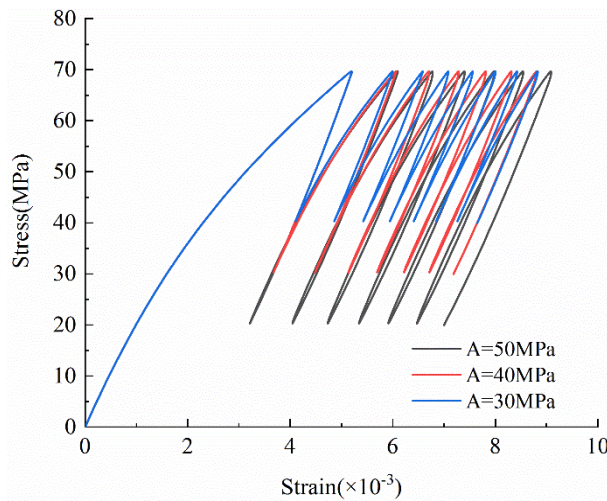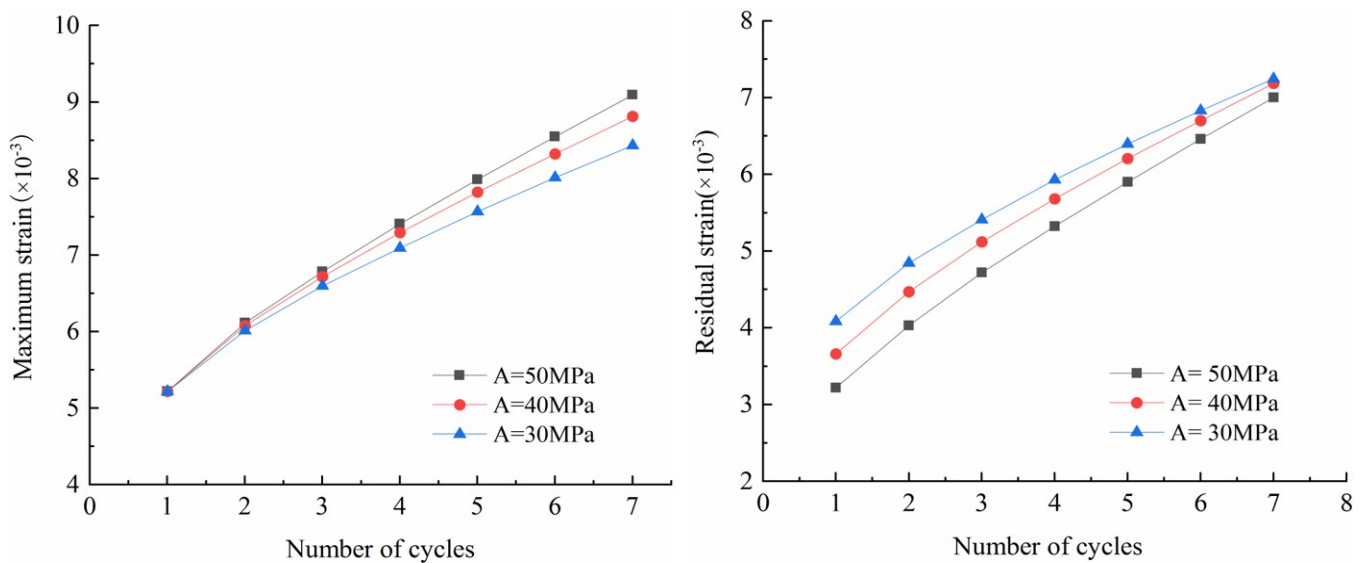

Figure 7. Stress–strain curves under different loading amplitudes

(a) Maximum strain with the number of cycles

(b) Residual strain with the number of cycles

Figure 8. Variation in strain with cycle times under different loading amplitudes

The influence of loading amplitude on rock deformation can also be explained by the rock fracturing mechanism: when the maximum stress is constant, the amplitude increases, and the corresponding minimum loading stress of the rock gradually decreases. The cracks in the rock are not easily extended as before, making it difficult to generate new cracks (Wang, YS et al., 2016). The expansion of the plastic zone is mainly due to the influence of the maximum load in the cyclic load on the rock, and the residual strain is mainly determined by the minimum loading stress. The endochronic plastic constitutive model proposed in this study can better reflect the phenomenon in which the residual strain of the rock gradually decreases with an increase in the amplitude when the maximum loading stress is fixed.

Numerical investigation of the effect of improved endochronic constitutive model on rock material deformation under cyclic loading

Jian Ming Huang et al.

4.3 Influence of confining pressure under cyclic loading

To fix the maximum loading stress and its amplitude, different degrees of confining pressure were applied to the rock to observe the deformation of the rock material. Three different confining pressures of 10, 20, and 30 MPa were selected for the experiment. The stress–strain curves are shown in Fig. 9. The maximum axial strain and residual strain of the rock under different confining pressures are shown in Fig. 10. As the confining pressure increased, the maximum axial strain and residual strain of the rock gradually decreased; in the fifth cycle, the maximum axial strain of the rock decreased from 0.004405 with a confining pressure of 10 MPa to 0.003010 with a confining pressure of 30 MPa. Moreover, the hysteresis loop in the stress–strain curve decreases gradually, which is consistent with the results in reference (Liu and He 2012).
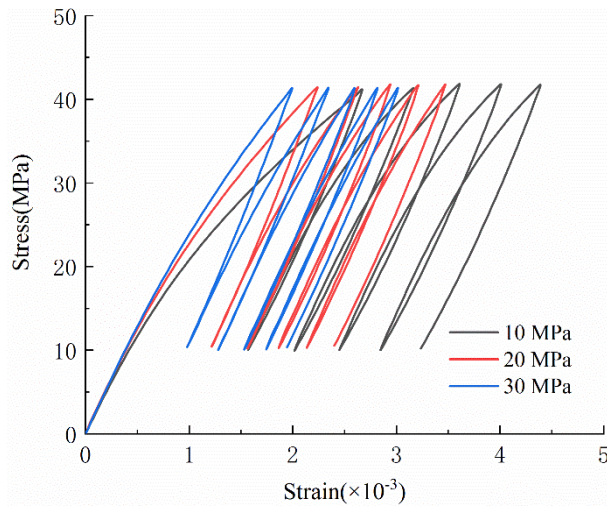

Figure 9. Stress–strain curves under different confining pressures

(a) Maximum strain with the number of cycles

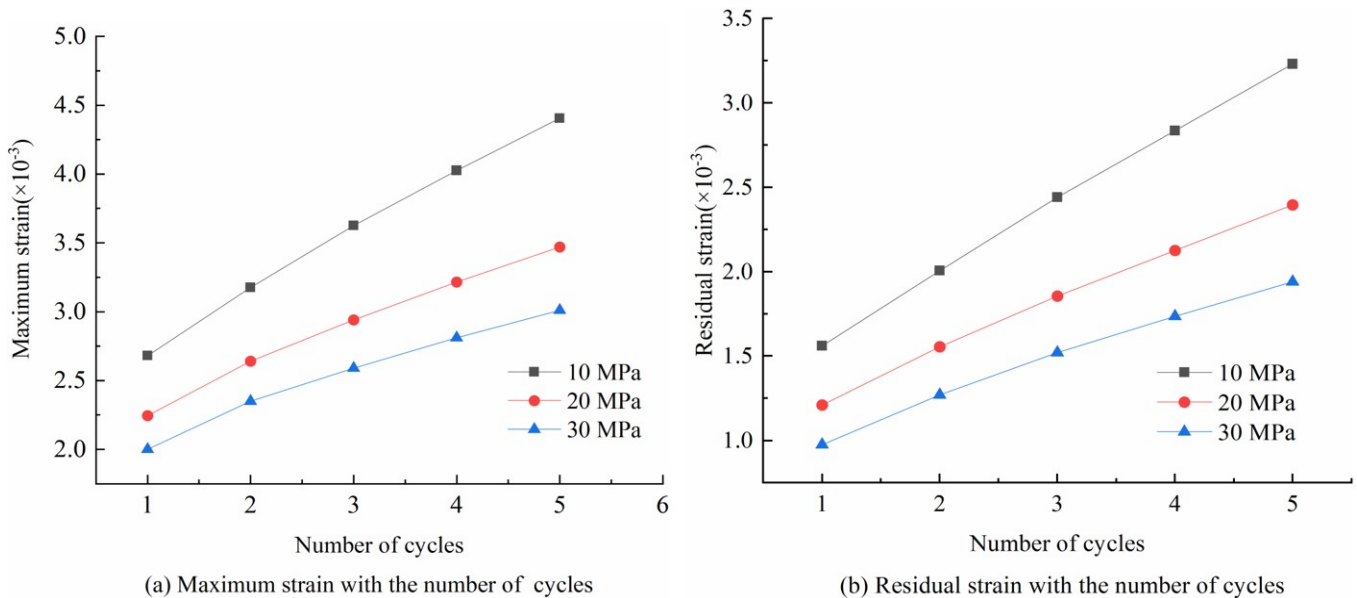(b) Residual strain with the number of cycles

Figure 10. Variation in strain with cycle times under different confining pressures
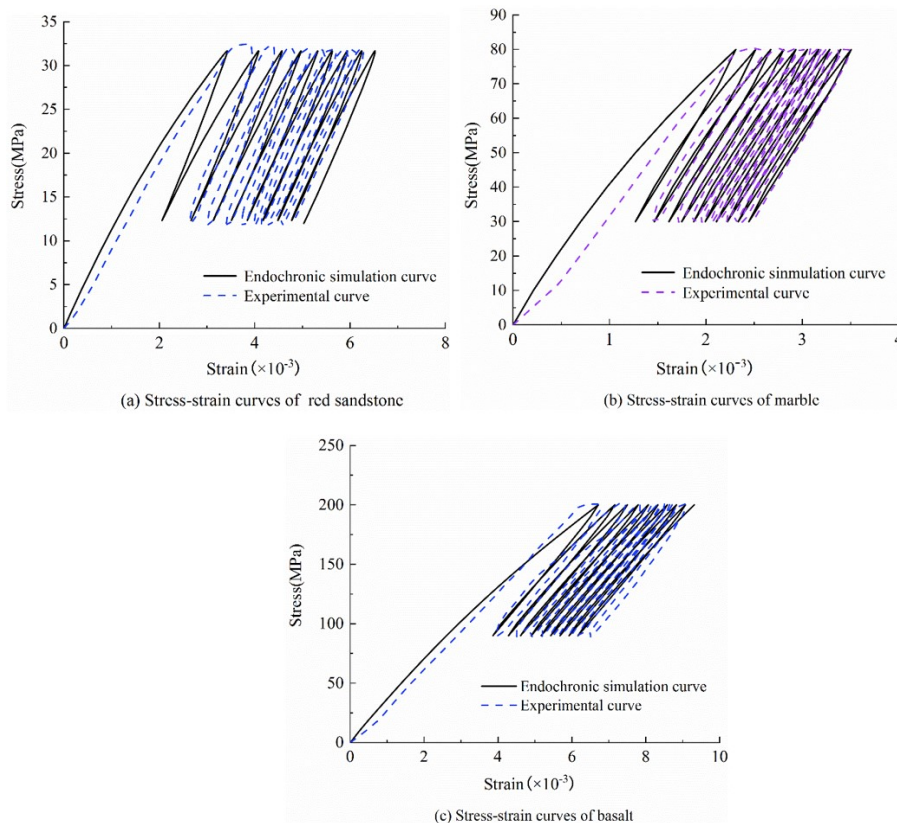
When the rock is subjected to constant-amplitude cyclic loading, the above-mentioned phenomena exhibited at different confining pressures can be explained by the failure mechanism of the rock under triaxial compression (Liu and He 2012). With the gradual increase in confining pressure, the expansion of internal cracks in the rock is restricted, and the compressive strength of the rock increases. Under a constant-amplitude load, the degree of deformation is relatively reduced.

Numerical investigation of the effect of improved endochronic constitutive model on rock material deformation under cyclic loading

Jian Ming Huang et al.

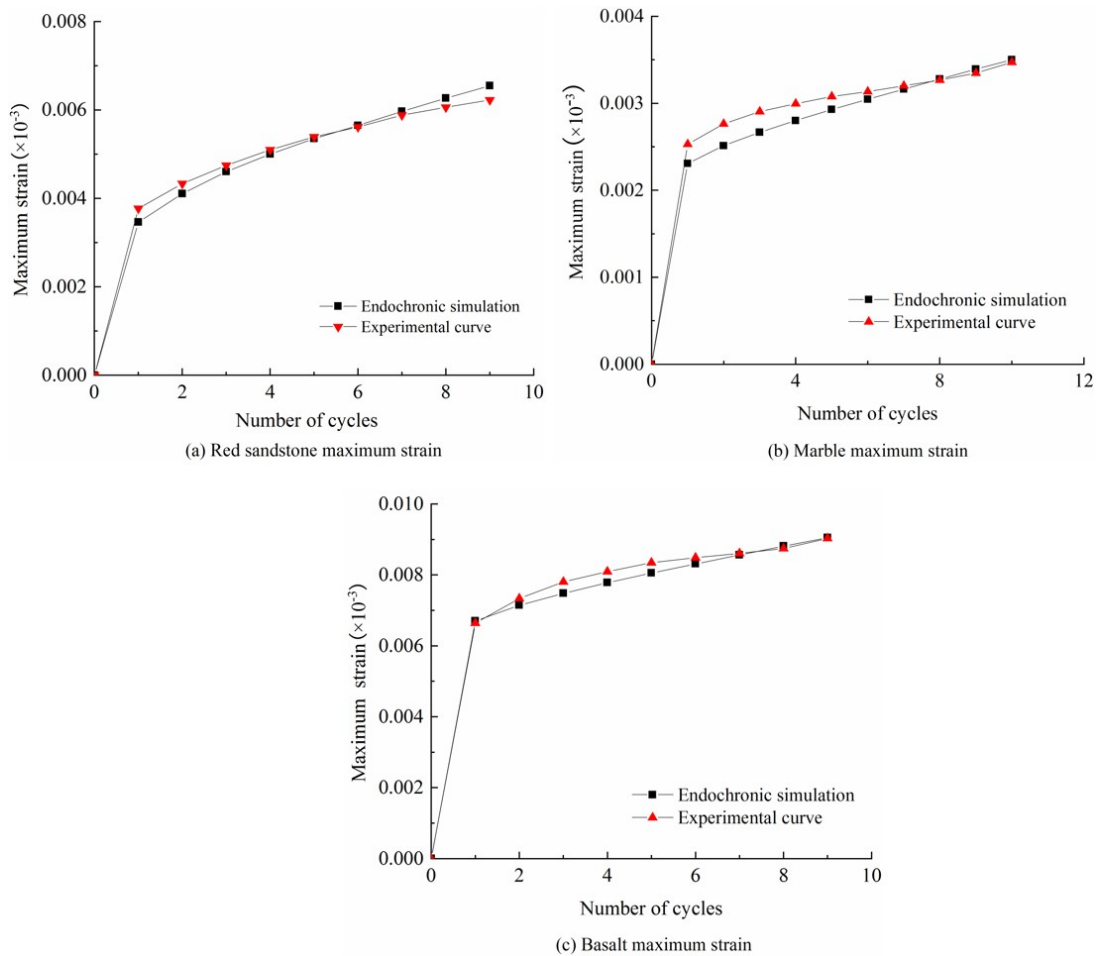## 4.4 Experimental verification of different rock types

Different rock types were selected for numerical simulation to verify the validity and reliability of the model. Experimental data for red sandstone, marble, and basalt from the literature were selected to verify the constitutive model (Ge 1987; Ge and Lu 1992; Zhou et al., 2019). Their parameters are listed in Table 2. The upper and lower limit stresses for red sandstone are 32 and 12 MPa, respectively; those for marble are 80 and 30 MPa, respectively; and those for basalt are 200 and 90 MPa, respectively. According to Fig. 11, one can see that, although three different rocks were selected, the endochronic model well reflects the deformation of different rocks under cyclic loading. For different rocks, the model transitions smoothly from the elastic stage to the elastoplastic stage. It well simulates the stiffness change of the rock during the loading process, and the cumulative plastic strain gradually increases according to the actual situation. The deformation of different kinds of rocks in the first cycle of the initial loading stage is shown in Fig. 11. The upper limit peak stress of the rock is relatively consistent with the experimental data, and the deformation of the rock increases rapidly in the first cycle, gradually diminishing during the subsequent cyclic load loading process. The relationship between the maximum axial strain and the number of cycles is shown in Fig. 12. The simulated axial strain of red sandstone in the first cycle is 0.003463, whereas the actual axial strain is 0.003772; the simulated axial strain of marble is 0.006703, whereas the actual axial strain is 0.006643; and the simulated axial strain of basalt is 0.002307, whereas the actual axial strain is 0.002529. The errors between the simulated and actual strain of the three types of rocks in the first loading cycle were 8.1%, 0.9%, and 8.7%, respectively, and all these errors were within the acceptable range. At the end of the cyclic loading process, the simulation data for the rock gradually coincide with the experimental data fitting. The simulated and actual axial strains of the three rocks in the last cycle were 0.006548, 0.009051, and 0.003501 and 0.006227, 0.009031, 0.003471, respectively, yielding errors of 4.9%, 0.2%, and 0.8%, respectively.

Table 2. Rock parameters

Rock type	E (Pa)	ν	u	β	M_i	α_i
Red stone	9.3×10^9	0.33	0.29	0.69	2.9×10^8	2×10^2
Marble	29×10^9	0.29	0.24	0.77	4.6×10^8	5.2×10^2
Basalt	32×10^9	0.2	0.18	0.85	7.2×10^8	7×10^2

(a) Stress-strain curves of red sandstone

(b) Stress-strain curves of marble

(c) Stress-strain curves of basalt

Figure 11. Comparison between experimental and simulation stress–strain curves for (a) red sandstone, (b) marble, and (c) basalt

Numerical investigation of the effect of improved endochronic constitutive model on rock material
deformation under cyclic loading

Jian Ming Huang et al.

Figure 12. Comparison between simulated and experimental maximum strains for (a) red sandstone, (b) marble, and (c) basalt

Under the action of cyclic loading, the deformation development rate of the rock was relatively fast during the initial loading stage and then gradually stabilized. The above simulation results are consistent with the experimental phenomenon reported in the literature (Ge and Lu 1992).

5 CONCLUSION

The study of the mechanical response and deformation mechanism of rock under cyclic loading is of great significance in engineering practice. In this study, we proposed a modified endochronic plasticity theory and numerically simulated the deformation of rock samples under cyclic loading. The endochronic plastic constitutive model has been used to study the deformation characteristics of rocks under different confining pressures, maximum loads, amplitudes, and rock types. The following conclusions can be made:

The value of β affected the width of the hysteresis loop, and, as the value of u decreased, the cumulative plastic strain of the curve increased and the plastic modulus decreased. The cumulative plastic strain was inversely proportional to u and directly proportional to the plastic modulus.

The improved endochronic constitutive model simulation can better simulate the Masing effect and ratchet effect of the rock under cyclic loading.

The modified endochronic plastic theory proposed improves the form of the strengthening function and reduces the number of model parameters. The improved constitutive model was verified by experiments on three different rocks,and the experimental results prove that the improved endochronic constitutive model can reflect the hysteresis curve and cumulative plastic deformation of the rock under cyclic loading.

The maximum axial strain and residual strain became linear as the maximum loading stress increased. At a fixed maximum loading stress but with different stress amplitudes applied, the maximum axial strain is basically unchanged, but the residual strain is inversely proportional to the amplitude. When different confining pressures were applied, the maximum axial strain was inversely proportional to the confining pressure, and the hysteresis area gradually decreased, but

Numerical investigation of the effect of improved endochronic constitutive model on rock material
deformation under cyclic loading

Jian Ming Huang et al.

its stiffness increased. The above-mentioned numerical simulation results are consistent with the experimental results, indicating that the improved endochronic constitutive model can better reflect the deformation characteristics of rock.

Author's Contributions: Conceptualization, W Zeng; Methodology, JM Huang and LJ Chen ; Formal analysis, JM Huang and X LIU; Validation, JM Huang and SL Hu; Writing – JM Huang,; Writing - review & editing, JM Huang and W Zeng.

Editor: Marcílio Alves

References

Khaledi, K. Mahmoudi, E. Datcheva, M et al. (2016). Stability and serviceability of underground energy storage caverns in rock salt subjected to mechanical cyclic loading. Int J Rock Mech Min Sci 86: 115–131.

Liu, Y. Dai, F. Zhao, T. Xu, N. (2017). Numerical investigation of the dynamic properties ofintermittent jointed rock models subjected to cyclic uniaxial compression. Rock Mech Rock Eng 50: 89–112.

Xiao J.Q. Ding D.X. Xu, G. Jiang F.L. (2009). Inverted S-shaped model for nonlinear fatigue damage of rock. International Journal of Rock Mechanics and Mining Sciences 46: 643-648

Attewell, PB. Farmer, IW. (1973). Fatigue behavior of rock.Int J Rock Mech Min Sci Geomech Abstr 10: 1–9.

Zhou, YQ. Sheng,Q. Li, NN. Fu, XD.(2015).Preliminary application of subloading surface to cyclic plastic model for rock under cyclic loading. Chinese Journal of Rock Mechanics and Engineering 34:2073-2082

M.N,Bagde. V.Petroš. (2005). Fatigue properties of intact sandstone samples subjected to dynamic uniaxial cyclical loading. Inte -rnational Journal of Rock Mechanics and Mining Sciences 42: 237-250.

Deng, H.Hu, Y.Li, J. Wang, Z. Zhang X, et al.(2017). Effect of frequency and amplitude of cyclic loading on the dynamic characteristics of sandstone. Rock Soil Mech 38: 3402-9

Liu, EL. Huang, R. He, S. (2012). Effects of frequency on the dynamic properties of intact rock samples subjected to cyclic loading under confining pressure conditions. Rock Mech Rock Eng 45: 89-102.

Fuenkajorn,K. Phueakphum, D. (2010). Effects of cyclic loading on mechanical properties of Maha Sarakham salt. Engineering Geology 112:43-52

GE, XR. JIANG, Y. LU, YD et al. (2003). Testing studyon fatigue deformation law of rock under cyclic loading. Chinese Journal of Rock Mechanics and Engineering 22: 1581-1585.

Xiao, J. Ding, D. Xu, G. Jiang F.L. (2007). Waveform effect on quasi-dynamic loading condition and the mechanical properties of brittle materials. Int J Rock Mech Min Sci 45: 621-626.

Liu, HY. Lu, SR. Zhang, LR. (2014). Dynamic damage constitutive model for persistent jointed rock mass based on combination model method. Chinese Journal of Geotechnical Engineering 36:1814-1821.

Di, Y. LIU, EL. Sun, P. Xiang,B. Zheng, QS. (2020). Mechanical properties and binary-medium constitutive model for semi-through jointed mudstone samples. International Journal of Rock Mechanics and Mining Sciences 132: 104376.

Zhou, YQ. Sheng,Q. Li, NN. Fu, XD. (2019). Numerical investigation of the deformation properties of rock materials subjected to cyclic compression by the finite element method. Soil Dynamics and Earthquake Engineering 126: 105795.

Carmeliet, J. Abeele KEVD. (2002). Application of the Preisach-Mayergoyz space model to analyze moisture effects on the nonlinear elastic reponse of rock. Geophys Res Lett 29:41-48

Lin, QB. Cao, P. Mao, SY. Ou CJ. Cao RH. (2020). Fatigue behaviour and constitutive model of yellow sandstone containing pre-existing surface crack under uniaxial cyclic loading. Theoretical and Applied Fracture Mechanics 109: 102776.

Valanis, KC. (1971). A theory of visco-plasticity without a yieldsurface. Archiwum Mechaniki Stosowanej 23:517-551.

Bazant, ZP. Shieh, CL. (1980). Hysteretic fracture endochronic theory for concrete. ASCE. Journal of the Engineering Mechanics Division 106: 929-950.

Wang, HL. Song, YP. (2007). Endochronic damage constitutive model for confined concrete. Engineering Mechanics 24:120-127.

Numerical investigation of the effect of improved endochronic constitutive model on rock material
deformation under cyclic loading

Jian Ming Huang et al.

Jeremiah M. Stache, John F. Peters, Youssef Hammi. Farshid Vahedifard. (2019). A kinematic hardening model based on endochronic theory for complex stress histories. Computers and Geotechnics 114:103117.

Yin,GZ. Wang, DG. Zhang, DM. (2009). Endchronic damage constitutive model of coal containing gas. Rock and Soil Mechanics 30: 885-889.

Shimbo, Taiki. (2017). Development and application of a dynamic XFEM for the seismic residual displacement analysis of an embankment. Soils Found 57: 357-370.

Tejchman, J. Bobinski, J. (1996).Continuous and discontinuous modeling of fracture inconcrete using FEM. Springer Science & Business Media, Springer,Berlin,Germany 161-2.

Xiong, Q. Chen, Z. Kang, J. Zhou, T. Zhang, W. (2017). Experimental and finite element study on seismic performance of the LCFST-D columns. J.Constr Steel Res 137: 119–34.

Cheng, XL.Li, YF. Wang, PG. Liu, ZX. Zhou, YD. (2020). Model tests and finite element analysis for vertically loaded anchors subjected to cyclic loads in soft clays. Computers and Geotechnics 119:103317.

Cheng, XL. Wang, TJ. Zhang, JX. Liu, ZX. Cheng, WL. (2021). Finite element analysis of cyclic lateral responses for large diameter monopiles in clays under different loading patterns. Computers and Geotechnics 134:104104.

Han, L. Wang, W. Zhao, X. (2008). Behavior of steel beam to concrete-filled SHS column frames: finite element model and verifications. Eng Struct 30: 1647-58.

Watanabe, O. Atluri, S N. (1985). A New Endochronic Approach to Computational Elasto-Plastic : Exa- mple of a Cyclically Loaded Cracked Plate. Appl.Mech 52: 857-864.

Li, CC. Fu, WS. (1991). Rock material damage constitutive equations based on endochronic theory concerning temperature effect. Rock and Soil Mechanics 12: 1-10.

Mo, HH. (1988). Investigation of Cyclic Loading Testing and Constitutive Relation of Rock. Chinese Journal of Geotechnical Engineenng 7: 215-224.

Zhang, PY. Xia, CC. Zhou, SW. Zhou Y. Hu, YS. (2015). A constitutive model for rock under cyclic loading and unloading. Rock and Soil Mechanics 36: 3354-3359.

Momeni, A. Karakus, M. Khanlari, GR. Heidari, M. (2015). Effects of cyclic loading on the mechanical properties of a granite. Int J Rock Mech MinSci 77: 89-96.

Ma, L. Liu, X. Wang, M. Xu, H. Hua, R et al. (2013). Experimental investigation of the mechanical properties of rock salt under triaxial cyclic loading. Int J Rock Mech Min Sci 62: 34-41.

Wang,Y. Li, CH. Han, JQ. (2020). On the effect of stress amplitude on fracture and energy evolution of pre-flawed granite under uniaxial increasing-amplitude fatigue loads. Engineering Fracture Mechanics 240: 107366.

Wang, YS. Ma, LJ. Fan, PX. Chen, Y. (2016). A fatigue damage model for rock salt considering the effects of loading frequency and amplitude. International Journal of Mining Science and Technology 26: 955-958.

Liu, EL. He, SM. (2012). Effects of cyclic dynamic loading on the mechanical properties of intact rock samples under confining pressure conditions. Engineering Geology 125: 81-91.

GE, XR. (1987). Study on deformation and strength characteristics of large-scale triaxial test sample of rock under cyclic loading. Rock and Soil Mechanics 8: 1-19.

Ge, XR. Lu, YF. (1992). Testing Study on fatigue damage and irreversible deformation law of rock under cyclic load. Chinese Journal of Geotechnical Engineenng 14: 56-60.